



Cite this: *New J. Chem.*, 2024, 48, 15307

## Synthesis and catalysis of a Co13 disk surrounded by vanadium–oxygen crown†

Yuji Kikukawa,  <sup>★a</sup> Isshin Yoshida, <sup>a</sup> Ryoji Mitsuhashi,  <sup>b</sup> Masaru Yamane<sup>a</sup> and Yoshihito Hayashi  <sup>★a</sup>

By the reaction of the binuclear cobalt-containing polyoxovanadate  $[\text{Co}_2(\text{H}_2\text{O})_2\text{V}_{10}\text{O}_{30}]^{6-}$  with methanol, a tridecanuclear cobalt containing polyoxovanadate,  $[\text{Co}_{13}(\text{OH})_6(\text{OCH}_3)_6\text{V}_{24}\text{O}_{72}]^{10-}$  (**Co13**), was synthesized. Single crystals suitable for X-ray crystallographic analysis were obtained as trimethylphenylammonium salts. The tridecanuclear cobalt core exhibited a planar disk structure and 24 vertex-sharing  $\text{VO}_4$  units surrounded the edge of the disk. This is the largest  $\text{VO}_4$ -based polyoxovanadate as far as we know. Compound **Co13** was stable in the solution state. Electrochemical analysis showed the possibility of **Co13** to act as an oxidation catalyst for alcohols. Compound **Co13** acted as a catalyst for oxidation of several alcohols. After the reaction, the **Co13** catalyst was retrieved by the addition of an excess amount of ethyl acetate and filtration. The structure of the catalyst was maintained and reused. The oxidation of not only aromatic but also aliphatic alcohols proceeded with **Co13**. Compound **Co13** showed catalytic performance for the oxidation of secondary alcohols even in the presence of alkenic and primary alcoholic functions.

Received 25th June 2024,  
Accepted 6th August 2024

DOI: 10.1039/d4nj02900c

[rsc.li/nic](http://rsc.li/nic)

## Introduction

Vanadium-oxygen species exist as multinuclear species, called polyoxovanadates in the aqueous solution, except for under strong acidic and strong basic conditions.<sup>1</sup> Octahedrally coordinated VO<sub>6</sub>-based decavanadates and tetrahedrally coordinated VO<sub>4</sub>-based oligomers are the dominant species in acidic and basic solutions, respectively. The VO<sub>4</sub>-based structures are bridged by the vertex-sharing oxygen atoms to form circular structures. The circular polyoxovanadates act as inorganic ligands with nucleophilicity to stabilize cationic species at the centre of the circles.<sup>2</sup> Protons and various metal cores stabilized by circular polyoxovanadates, such as [HV<sub>4</sub>O<sub>12</sub>]<sup>3-</sup>, [PdV<sub>6</sub>O<sub>18</sub>]<sup>4-</sup>, [Cu<sub>2</sub>V<sub>8</sub>O<sub>24</sub>]<sup>4-</sup>, [Ni<sub>4</sub>V<sub>10</sub>O<sub>30</sub>(OH)<sub>2</sub>(H<sub>2</sub>O)<sub>6</sub>]<sup>4-</sup> (**Ni4**), [Mn<sub>2</sub>(V<sub>5</sub>O<sub>15</sub>)<sub>2</sub>]<sup>6-</sup>, [Co<sub>2</sub>(H<sub>2</sub>O)<sub>2</sub>V<sub>10</sub>O<sub>30</sub>]<sup>6-</sup> (**Co2**, Fig. 1), [(H<sub>2</sub>O)M(V<sub>4</sub>O<sub>12</sub>)<sub>2</sub>]<sup>5-</sup> (M = Y, Ho), [LnV<sub>9</sub>O<sub>27</sub>]<sup>6-</sup> (Ln = Ce, Pr, Nd, Sm, Eu, Gd, Tb, Dy), and [LnV<sub>10</sub>O<sub>30</sub>]<sup>7-</sup> (Ln = La, Er, Tm, Yb, Lu), were reported.<sup>2-8</sup> Although the obtained structures showed versatility, the synthetic procedures are almost the same. Tetravanadate [V<sub>4</sub>O<sub>12</sub>]<sup>4-</sup> is dissolved in an organic solvent and the addition of metal cations gives the metal-containing polyoxovanadates. Tetravanadate easily changes the number of VO<sub>4</sub> units and the

conformations of the rings.<sup>9</sup> In comparison with the general organic ligands, circular polyoxovanadate ligands show high flexibility as if the ligands adjust their own structures to the central core structures. Lanthanide-surrounding polyoxovanadates vary the conformations depending on the ionic radii.<sup>6,7</sup> In the case of manganese and cobalt, the number of manganese and cobalt cations increased by the reaction of the additional metal cations to form  $[\text{M}_3(\text{H}_2\text{O})\text{OAcV}_{10}\text{O}_{30}]^{5-}$  ( $\text{M} = \text{Co}(\text{Co3})$ ,  $\text{Mn}$ ,  $\text{OAc} = \text{acetate}$ ) and  $[\text{Mn}_6\text{O}_6\text{V}_8\text{O}_{26}(\text{OAc})_2]^{6-}$ .<sup>10,11</sup>

Layered cobalt oxides and hydroxides have attracted attention for application in sustainable and renewable energy generation and storage, superconductors, and catalysts.<sup>12–15</sup> The

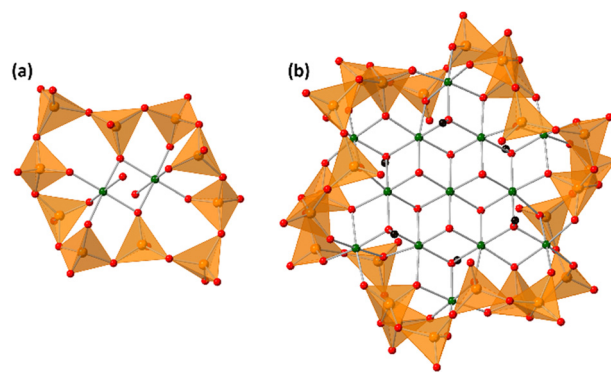


**Fig. 1** Anion structures of (a) **Co2** and (b) **Co13**. The green, orange, red, and black spheres represent cobalt, vanadium, oxygen, and carbon atoms, respectively. Orange tetrahedra represent  $\text{VO}_4$  units.

<sup>a</sup>Department of Chemistry, Graduate School of Natural Science and Technology,  
Kanazawa University, Kakuma, Kanazawa 920-1192, Japan.  
E-mail: kikukawa@se.kanazawa-u.ac.jp

<sup>b</sup> *Institute of Liberal Arts and Science, Kanazawa University, Kakuma, Kanazawa 920-1192, Japan*

† Electronic supplementary information (ESI) available. CCDC 2364056. For ESI and crystallographic data in CIF or other electronic format see DOI: <https://doi.org/10.1039/d4nj02900c>

separation of the monolayers produced a hydroxide ion conductor and electrochemical catalysts, especially for water splitting.<sup>16</sup> To prepare discrete monolayers, peeling reagents and/or protecting ligands for the flat surface of monolayers are important.<sup>17,18</sup> In these cases, the monolayers show size distribution. With the appropriate ligands surrounding the edge of the monolayer, single species were obtained. Up to now, planar multinuclear cobalt–oxygen complexes have been reported.<sup>19</sup> Planar heptanuclear cobalt hydroxide stabilized with functionalized 6-methoxyphenoxides showed the unique electron transfer, and it was used as an oxidation catalyst.<sup>19,20</sup> With isobutyrate and *N*-butyldiethanolamine, a decanuclear cobalt disk was synthesized. The disk contained both bridging hydroxide and alkoxide ligands.<sup>21</sup> By the reaction of cobalt sources with tris(hydroxymethyl)alkane, hepta- and tridecanuclear cobalt disks were prepared.<sup>22,23</sup> Triazacyclononane (tacn) also acted as a terminal ligand. Terminal mononuclear cobalt–tacn complexes were prepared in the first step. Then, the coordination of 6 monomers to the heptanuclear cobalt core afforded the tridecanuclear cobalt disk under basic media. The terminal ligands prevented further hydrolysis.<sup>24</sup> Not only organic ligands but also rigid polyoxometalates can stabilize the planar cobalt cores, such as  $[\text{Co}_4(\text{H}_2\text{O})_2(\text{XW}_9\text{O}_{34})_2]^{10-}$  ( $\text{X} = \text{P}, \text{V}$ ) and  $[\text{Co}_4(\text{OH})_2(\text{H}_2\text{O})_6(\text{H}_2\text{SiW}_{10}\text{O}_{36})_2]^{6-}$ .<sup>25–28</sup> Compound  $[\text{Co}_4(\text{H}_2\text{O})_2(\text{XW}_9\text{O}_{34})_2]^{10-}$  acted as an efficient homogeneous water oxidation catalyst. In this work, synthesis of a multinuclear cobalt disk surrounded by  $\text{VO}_4$ -based polyoxovanadate and its catalytic properties for alcohol oxidation were investigated.

## Results and discussion

### Synthesis of tridecanuclear cobalt containing polyoxovanadate

The solid of the previously reported binuclear cobalt containing polyoxovanadate **Co2** showed water-induced thermochromism.<sup>5</sup> The original colour of **Co2** was light green and, by exposure to water vapor, the solid colour changed to brown and, by heating to evaporate the adsorbed water, the light green colour was retrieved.<sup>5</sup> This result inspired us to investigate the colour change by addition of a substrate to the **Co2** solution. Methanol or 2-propanol was added to the acetonitrile solution of **Co2**. In the case of methanol, the solution colour changed from green to brown. Addition of 2-propanol caused no colour change. From the mixed solution of acetonitrile and methanol, tiny amounts of brown crystals were obtained. The IR spectrum of the crystalline sample was different from that of **Co2**, indicating the structure conversion (Fig. S1, ESI†). Although the quality of the crystals was too low to complete the X-ray crystallographic analysis, the anion structure was confirmed. It contained a tridecanuclear cobalt disk surrounded by 24  $\text{VO}_4$  units (**Co13**, Fig. 1). To improve the yield, triethylamine was added to the synthetic solution to assist the proton removal of methanol. The product **Co13** was selectively precipitated from the synthetic solution. The low yield of **Co13** was due to the unidentified by-products in the solution. The yield clearly increased with increasing the amount of added triethylamine, while an excess amount of triethylamine caused impurities. After dissolution of 200 mg of **Co2**

in 0.8 mL of the mixed solvent of acetonitrile and methanol (3 : 1, v/v), addition of 2, 3, 4, and 5 equiv. of triethylamine with respect to **Co2** and allowing the solution to stand for 3 days at room temperature yielded 5.5, 9.4, 13, and 14 mg of the product, respectively. Under the optimized conditions, the yield reached 24%. From the elemental analysis and thermogravimetric analysis, the formula of the product was  $(\text{Et}_4\text{N})_5(\text{HEt}_3\text{N})_5[\text{Co}_{13}(\text{OH})_6(\text{OCH}_3)_6\text{V}_{24}\text{O}_{72}]\cdot 10\text{H}_2\text{O}$ . From the electrospray ionization mass spectrometry (ESI-MS) spectrum, the corresponding ion pairs due to **Co13** were observed (Fig. S2, ESI†). The distribution of the ion pairs indicates that the bridging methoxide ligands and/or hydroxide ligands are exchangeable.

Single crystals suitable for X-ray crystallographic analysis were obtained by the cation exchange to trimethylphenylammonium. The IR spectra in the fingerprint region of polyoxovanadates were the same between ethylammonium salts and trimethylphenylammonium salts, showing that the anion structure was maintained during the cation exchange (Fig. S1, ESI†). The BVS values of cobalt and vanadium atoms were 2.00–2.10 and 4.96–5.17, showing cobalt and vanadium atoms were divalent and pentavalent, respectively.<sup>29</sup> Oxygen atoms surrounding the centred cobalt atom were hydroxide ligands. They bridged the centred cobalt atom and 6 cobalt atoms. The 6 cobalt atoms were bridged by methoxide ligands. The methyl groups were located vertically to the tridecanuclear cobalt disk, and the directions were opposite to the next methoxide ligands. Methoxide ligands also bonded to the outer 6 cobalt atoms. The arrangement of the 13 cobalt atoms was similar to that of  $[\text{Co}_{13}(\text{OH})_{24}(\text{tacn})_6]^{8+}$ .<sup>24</sup> The tridecanuclear cobalt disk was surrounded by the  $[\text{V}_{24}\text{O}_{72}]^{24-}$  crown. The crown was composed of 24 vertex-sharing  $\text{VO}_4$  units. The 48 membered  $\text{V}_{24}\text{O}_{24}$  ring could be drawn with a single stroke. The top view of the ring represented a gear shape (Fig. 2). The side view of the ring contained three waves. The numbers of waves of the surrounding polyoxovanadate ligands in **Co2** and **Co3** were 5 and 4, respectively.<sup>10</sup> With increasing number of cobalt atoms in the crown, the number of waves of the vanadium–oxygen ring decreased (Fig. 2). The conformation relationship between the central disk and surrounding polyoxovanadate crowns in **Co13** was different from that in previously reported planar core-containing polyoxovanadate **Ni4**.<sup>4</sup> The polyoxovanadate crown of **Co13** was located in the same plane as the tridecanuclear cobalt disk, while the crown of **Ni4** was perpendicular to the tetranuclear nickel plane.

The direct current magnetic measurement of the trimethylphenylammonium salts of **Co13** was carried out using the crystalline sample. The  $\chi_{\text{MT}}$  value of  $48.3 \text{ cm}^3 \text{ K mol}^{-1}$  was much larger than the value calculated from the spin-only equation for 13 high-spin  $\text{Co}^{\text{II}}$  ions ( $24.4 \text{ cm}^3 \text{ K mol}^{-1}$ ) due to the significant spin–orbit coupling of the octahedral  $\text{Co}^{\text{II}}$  ion (Fig. S3, ESI†). The  $\chi_{\text{MT}}$  value gradually decreased to a minimum at 34 K and slightly increased to reach a value of  $40.1 \text{ cm}^3 \text{ K mol}^{-1}$  at 19 K. Upon further cooling, the  $\chi_{\text{MT}}$  abruptly decreased down to  $24.6 \text{ cm}^3 \text{ K mol}^{-1}$ . The slight increase at 34 K can be attributed to the ferromagnetic exchange coupling between  $\text{Co}^{\text{II}}$  centers. This feature competed

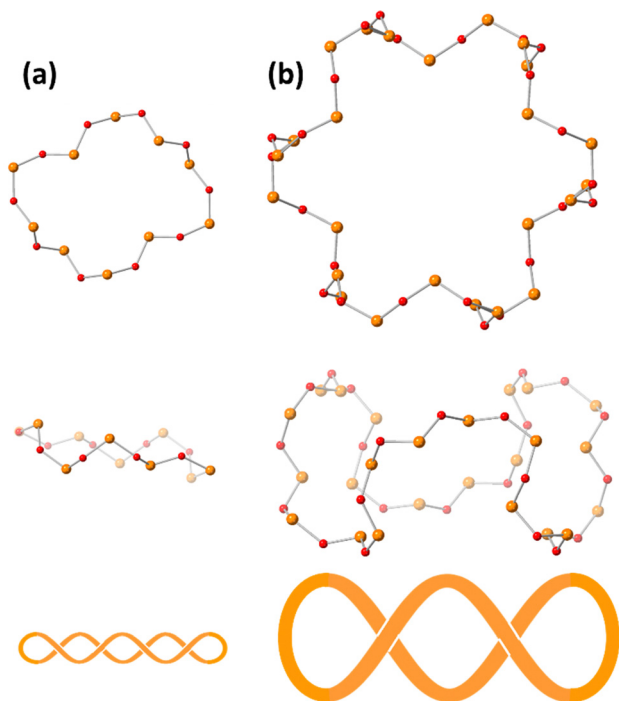


Fig. 2 Top and side views and schematic representations of (a) the  $V_{10}O_{10}$  ring in **Co2** and (b) the  $V_{24}O_{24}$  ring in **Co13**. The orange and red spheres represent vanadium and oxygen atoms, respectively.

with the sharp decrease owing to the zero-field splitting. The alternating current susceptibility measurement was performed to observe slow magnetic relaxation behavior. However, no frequency dependence was observed for the out-of-phase signal ( $\chi''_M$ ), indicating that **Co13** is not a single-molecule magnet (Fig. S4, ESI†).

### Oxidation properties

The electrochemical properties of **Co13** were investigated. In the range of 0–2.0 V vs. ferrocene/ferrocenium ( $Fc/Fc^+$ ), a weak and broad oxidation peak around 1.5 V was observed. By the addition of methanol, an increase of the catalytic current over 1.0 V was observed. In addition, an irreversible oxidation peak at 1.5 V was clearly observed (Fig. 3). The IR spectra show that the **Co13** structure is maintained after treatment with an excess amount of methanol in the solution state (Fig. S5, ESI†). Without **Co13** or with a typical metavanadate,  $[V_4O_{12}]^{4-}$ , the current increase was not observed. With  $Co(NO_3)_2$ , the catalytic current increase was observed over 1.4 V without a peak top (Fig. S6, ESI†). With **Co2**, addition of methanol caused the decomposition of the structure. The second cycle of **Co13** solution with methanol showed a weak current probably due to the adsorption of the inactive species on the surface of the electrode (Fig. S7, ESI†). In the case of water addition to the **Co13** solution, the peak current over 1.0 V increased (Fig. S8, ESI†). Addition of non-oxidative *tert*-butyl alcohol did not show the current increase (Fig. S8, ESI†). After the treatment of 5000 equiv. of water or 10 000 equiv. of *tert*-butyl alcohol, the **Co13** structure was maintained (Fig. S5, ESI†).

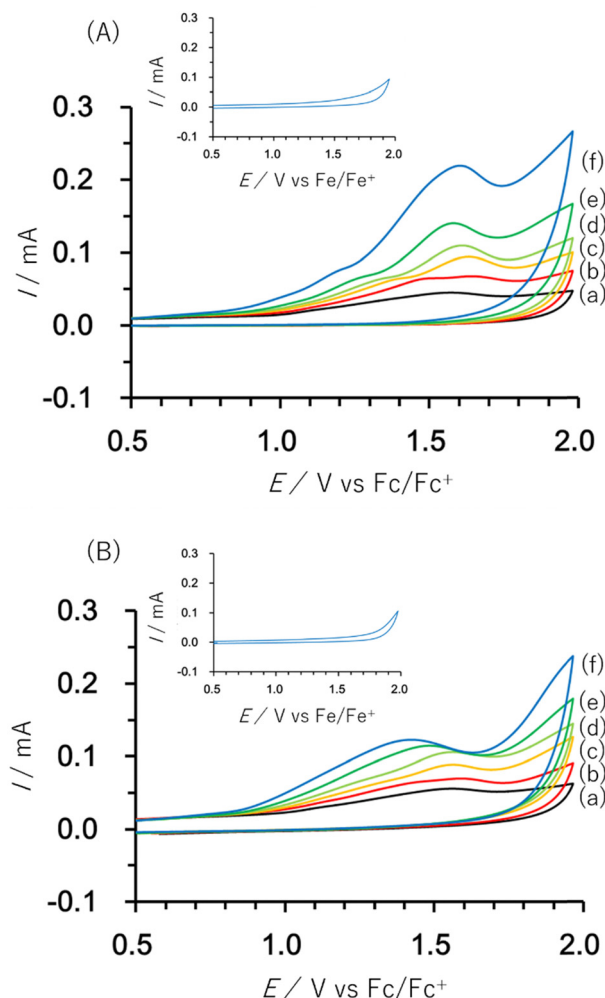


Fig. 3 First cycle of cyclic voltammograms of **Co13** in the presence of (a) 0 equiv., (b) 100 equiv., (c) 300 equiv., (d) 500 equiv., (e) 1000 equiv., and (f) 3000 equiv. of (A) methanol and (B) 1-butanol. The insets show voltammograms under the condition (f) without **Co13**.

By the addition of 1-butanol to the **Co13** solution, the peak top potential shifted to 1.4 V, indicating the ligand exchange (Fig. 3). The IR spectra also supported the ligand exchange (Fig. S9, ESI†). After the reaction with 1-butanol, 2-butanol, and benzyl alcohol, the peak at  $860\text{ cm}^{-1}$  of the original **Co13** shifted to 843, 847, and  $853\text{ cm}^{-1}$ , respectively. In the case of bulky *tert*-butyl alcohol, no peak shift was observed (Fig. S5, ESI†). After the constant potential electrolysis at 1.5 V in the presence of 1-butanol with **Co13**, a trace amount of butanal was detected by the GC–MS measurement.

Next, chemical oxidation of alcohols was investigated (Table 1). *tert*-Butyl hydroperoxide (TBHP) was used as an oxidant. The IR spectrum of the solid collected by filtration after the addition of ethyl acetate into the **Co13** solution in the presence of 500 equiv. of TBHP was identical to that of the original samples of **Co13**, showing the stability of **Co13** towards TBHP (Fig. S10, ESI†). The reaction was carried out in the mixed solvent of propylene carbonate and acetonitrile (1:1, v/v) to dissolve the catalysts. With **Co13** as a catalyst, oxidation of

Table 1 Oxidation of various alcohols<sup>a</sup>

Entry	Substrate	Product	Catalyst ( $\mu\text{mol}$ )	Time/h	Conversion/%	Yield/%
1			<b>Co13</b> (2)	24	99	99
2			$\text{Co}(\text{NO}_3)_2$ (26)	24	45	45
3			<b>Co2</b> (13)	24	91	88
4			$\{\text{Et}_4\text{N}\}_4[\text{V}_4\text{O}_{12}]$ (12)	24	93	93
5			$\text{Co}(\text{NO}_3)_2$ (26) $\{\text{Et}_4\text{N}\}_4[\text{V}_4\text{O}_{12}]$ (12)	24	78	78
6			—	24	8	7
7			<b>Co13</b> (2)	36	96	95
8	R = <i>p</i> -Me	R = <i>p</i> -Me	<b>Co13</b> (2)	36	95	92
9	R = <i>p</i> -Cl	R = <i>p</i> -Cl	<b>Co13</b> (2)	36	99	99
10	R = <i>m</i> -NO <sub>2</sub>	R = <i>m</i> -NO <sub>2</sub>	<b>Co13</b> (2)	36	98	98
11			<b>Co13</b> (2)	35	94	94
12			<b>Co13</b> (2)	2	33	32
13			$\{\text{Et}_4\text{N}\}_4[\text{V}_4\text{O}_{12}]$ (12)	2	24	15
14			<b>Co13</b> (2)	24	54	54
15			<b>Co13</b> (2)	21	46	46
16 <sup>b</sup>			<b>Co13</b> (2)	10	44	29
17 <sup>c</sup>			<b>Co13</b> (2)	10	71	47

<sup>a</sup> Reaction conditions: substrate (1 mmol), catalysts (2–26  $\mu\text{mol}$ ), 5.5 M of TBHP in decan (1 mmol), acetonitrile (1 mL), propylene carbonate (1 mL), internal standard (0.2 mmol), 32 °C, 800 rpm with a Teflon-coated magnetic stirrer bar. Conversion and yields were determined by GC.

<sup>b</sup> The primary alcohol oxidation product was not detected. <sup>c</sup> The alcohol was selectively oxidized without the formation of epoxide.

diphenyl methanol proceeded smoothly to afford the corresponding ketone in 99% yield in 24 h (entry 1).

After the reaction, the catalyst was collected by filtration after the addition of an excess amount of ethyl acetate. The IR spectrum of the retrieved catalyst was the same as those of the original samples (Fig. S11, ESI<sup>†</sup>). The ESI-MS spectrum of the retrieved catalyst showed the related peak sets of **Co13** (Fig. S12, ESI<sup>†</sup>). The retrieved catalyst was reused for alcohol oxidation. The oxidation of diphenyl methanol with the retrieved catalyst gave a 93% yield (Fig. S13, ESI<sup>†</sup>). The reactivity of  $\text{Co}(\text{NO}_3)_2$  was lower than that of **Co13** (entry 2). Although the reactivities of **Co2** and  $[\text{V}_4\text{O}_{12}]^{4-}$  were similar to that of **Co13**, their structures were decomposed during the reaction (entries 3 and 4; Fig. S14 and S15, ESI<sup>†</sup>). The second run with retrieved catalysts of **Co2** and  $[\text{V}_4\text{O}_{12}]^{4-}$  gave lower yields (Fig. S13, ESI<sup>†</sup>). The simple mixture of  $\text{Co}(\text{NO}_3)_2$  and  $[\text{V}_4\text{O}_{12}]^{4-}$  gave a medium yield of the product (entry 5). Without catalysts, the reaction hardly proceeded (entry 6). The oxidation of 1-phenyl ethanol and its derivatives smoothly proceeded to give the corresponding acetophenone derivatives (entries 7–10). The derivatives with both electron donating and electron accepting groups were efficiently oxidized. The oxidation of the radical-clock substrate exclusively produced cyclopropyl phenyl ketone without ring-opening products, indicating that free-radical

intermediates were not involved in the present alcohol oxidation (entry 11).<sup>30</sup> The oxidation of benzyl alcohol with **Co13** gave a higher yield of benzaldehyde than that with  $[\text{V}_4\text{O}_{12}]^{4-}$  in 2 h, although the yield was low due to substrate inhibition (entries 12 and 13, Fig. S9, ESI<sup>†</sup>). The oxidation reactions of cyclic and linear aliphatic alcohols proceeded to afford the corresponding aliphatic ketones with medium yields with stopping the reactions probably due to the inhibition of substrates by the coordination to active centres (entries 14–17). The alcohol oxidation with **Co13** was secondary selective. The oxidation of 1,3-butanediol selectively took place at the secondary position (entry 16). 2-Cyclohexene-1-ol possesses two oxidative functions. In the presence of **Co13**, alcohol oxidation selectively proceeded without the formation of epoxy products (entry 17). The oxidative product observed in the GC chart was only 2-cyclohexene-1-one.

After the treatment of **Co13** with TBHP, the IR peak at  $860\text{ cm}^{-1}$  was slightly shifted, indicating the coordination of TBHP (Fig. S10, ESI<sup>†</sup>). The isolated samples after the treatment with TBHP were utilized for the oxidation of diphenyl methanol. Without an additional oxidant, *ca.* 6 equiv. of benzophenone was obtained, showing the coordination of TBHP to **Co13** was included in the reaction paths. In the previous work, it was reported that a tetrahedrally coordinated vanadium centre has



the potential to activate TBHP.<sup>31</sup> Based on the results reported herein and previous reports, we propose the possible reaction paths. The oxidant TBHP was activated by the coordination to vanadium and/or cobalt centres. The approach of the substrates to the activated TBHP gives the products.

## Experimental

### Materials

All reagents were obtained from commercial suppliers and used without further purification unless otherwise noted.  $\{\text{Et}_4\text{N}\}_4[\text{V}_4\text{O}_{12}]$  and  $\{\text{Et}_4\text{N}\}_6[\text{Co}_2(\text{H}_2\text{O})_2\text{V}_{10}\text{O}_{30}]$  (**Co2**) were synthesized following the literature method.<sup>5,32</sup> 7-Oxabicyclo[4.1.0]heptan-2-ol (2,3-epoxycyclohexanol) was obtained with the previously reported system with  $\{n\text{-Bu}_4\text{N}\}_5[\text{V}_{18}\text{O}_{46}(\text{NO}_3)]^{5-}$ .<sup>33</sup>

### Synthesis of the tridecanuclear cobalt-containing polyoxovanadate $[\text{Co}_{13}(\text{OH})_6(\text{OCH}_3)_6\text{V}_{24}\text{O}_{72}]^{10-}$ (**Co13**)

$\{\text{Et}_4\text{N}\}_6[\text{Co}_2(\text{H}_2\text{O})_2\text{V}_{10}\text{O}_{30}]$  200 mg (0.10 mmol) was dissolved in 0.8 mL of the mixed solvent of acetonitrile and methanol (3 : 1, v/v). After the addition of 58  $\mu\text{L}$  triethylamine (0.40 mmol), the solution was stirred for 1 h. Then the solution was filtered to remove the insoluble materials. The solution was kept standing for 2 days at 35 °C. **Co13** (21 mg) was obtained as a brown powder (24% yield based on cobalt). Elemental analysis calcd for  $\{\text{Et}_4\text{N}\}_6\{\text{Et}_3\text{HN}\}_4[\text{Co}_{13}(\text{OH})_6(\text{OCH}_3)_6\text{V}_{24}\text{O}_{72}] \cdot 12\text{H}_2\text{O}$ : C 19.37%, H 4.84%, N 2.90%; found: C 19.44%, H 4.61%, N 2.82%. Ethylammonium salts of **Co13** were used for the electrochemical analysis and catalytic reactions. The crystalline samples suitable for the single crystal X-ray analysis were obtained by cation exchange. **Co13** and 100 equiv. of trimethylphenylammonium bromide with respect to **Co13** were dissolved in DMSO at 60 °C. Vapor diffusion of ethyl acetate to the **Co13** solution at 35 °C gave red crystals. Elemental analysis calcd for  $\{\text{Me}_3\text{PhN}\}_{10}[\text{Co}_{13}(\text{OH})_6(\text{OCH}_3)_6\text{V}_{24}\text{O}_{72}] \cdot 4\text{Me}_2\text{SO} \cdot 10\text{H}_2\text{O}$ : C 23.64%, H 3.97%, N 2.65%, S 2.43%; found: C 23.37%, H 3.99%, N 2.60%, S 2.45%. CCDC 2364056 contains the supplementary crystallographic data for **Co13** (Table S1, ESI<sup>†</sup>).

## Conclusions

Methanol-induced structure conversion from binuclear to tridecanuclear cobalt-containing polyoxovanadates under basic conditions was discovered by monitoring the colour change of the solution with additives. Among cobalt-containing  $\text{VO}_4$ -based polyoxovanadate crowns, the numbers of waves in the V–O rings decrease with increasing number of central cobalt atoms. Compound **Co13** acted as an oxidation catalyst for the alcohol. The ligand exchanges might assist the oxidation reactions. The size and conformation of polyoxovanadate crowns were controllable to adjust the central metal cores. Conversion of the central metal core structures induces structure dependent properties. Polyoxovanadate crowns are some of the candidates to support such phenomena.

## Author contributions

Y. K.: conceptualization, funding acquisition; R. M.: characterization; I. Y.: spectroscopic analysis and catalytic reactions; M. Y.: synthesis and electrochemistry; Y. K. and Y. H.: supervision. All authors have contributed to writing of the manuscript.

## Data availability

Crystallographic data for **Co13** have been deposited at CCDC under 2364056 and can be obtained from <https://www.ccdc.cam.ac.uk/>.

## Conflicts of interest

There are no conflicts to declare.

## Acknowledgements

We thank Mr H. Aihara for the preliminary experiments. This research was partly supported by the JSPS KAKENHI Grant No. JP23H04621 and JP23K04776, JSPS Core-to-Core program, and the JST FOREST Program Grant No. JPMJFR2023720466.

## Notes and references

- 1 C. F. Baes and R. E. Mesmer, *The hydrolysis of cations*, John Wiley, New York, 1976.
- 2 Y. Hayashi, *Coord. Chem. Rev.*, 2011, **255**, 2270.
- 3 J. Fuchs, S. Mahjour and J. Pickardt, *Angew. Chem., Int. Ed. Engl.*, 1976, **15**, 374.
- 4 T. Kurata, A. Uehara, Y. Hayashi and K. Isobe, *Inorg. Chem.*, 2005, **44**, 2524.
- 5 S. Inami, M. Nishio, Y. Hayashi, K. Isobe, H. Kameda and T. Shimoda, *Eur. J. Inorg. Chem.*, 2009, 5253.
- 6 M. Nishio, S. Inami, M. Katayama, K. Ozutsumi and Y. Hayashi, *Inorg. Chem.*, 2012, **51**, 784.
- 7 M. Nishio, S. Inami and Y. Hayashi, *Eur. J. Inorg. Chem.*, 2013, 1876.
- 8 T. Maruyama, H. Kawabata, Y. Kikukawa and Y. Hayashi, *Eur. J. Inorg. Chem.*, 2019, 529.
- 9 Y. Kikukawa, H. Kawabata and Y. Hayashi, *RSC Adv.*, 2021, **11**, 31688.
- 10 T. Maruyama, Y. Kikukawa, H. Sakiyama, M. Katayama, Y. Inada and Y. Hayashi, *RSC Adv.*, 2017, **7**, 37666.
- 11 T. Maruyama, A. Namekata, H. Sakiyama, Y. Kikukawa and Y. Hayashi, *New J. Chem.*, 2019, **43**, 17703.
- 12 Y. Zhang and H. Ohta, *NPG Asia Mater.*, 2023, **15**, 67.
- 13 Y. Lyu, X. Wu, K. Wang, Z. Feng, T. Cheng, Y. Liu, M. Wang, R. Chen, L. Xu, J. Zhou, Y. Lu and B. Guo, *Adv. Energy Mater.*, 2021, **11**, 2000982.
- 14 J. V. Badding, *Nat. Mater.*, 2003, **2**, 208.
- 15 G. Chen, H. Wan, W. Ma, N. Zhang, Y. Cao, X. Liu, J. Wang and R. Ma, *Adv. Energy Mater.*, 2020, **10**, 1902535.
- 16 G. Song and X. Hu, *Nat. Commun.*, 2014, **5**, 4477.

- 17 R. Ma, Z. Liu, L. Li, N. Iyi and T. Sasaki, *J. Mater. Chem.*, 2006, **16**, 3809.
- 18 N. Tarutani, S. Kimura, T. Sakata, K. Suzuki, K. Katagiri and K. Inumaru, *ACS Mater. Lett.*, 2022, **4**, 1430.
- 19 A. M. Ulman and D. F. Nocera, *J. Am. Chem. Soc.*, 2013, **135**, 15053.
- 20 T. S. Mahapatra, D. Basak, S. Chand, J. Lengyel, M. Shatruk, V. Bertolasi and D. Ray, *Dalton Trans.*, 2016, **45**, 13576.
- 21 S. Schmitz, T. Secker, M. Batool, J. van Leusen, M. A. Nadee and P. Kögerler, *Inorg. Chim. Acta*, 2018, **482**, 522.
- 22 K.-D. Leng, S.-K. Xing, R. Herchel, J.-L. Liu and M.-L. Tong, *Inorg. Chem.*, 2014, **53**, 5458.
- 23 Y. Peng, C.-B. Tian, Y.-H. Lan, N. Magnani, Q.-P. Li, H.-B. Zhang, A. K. Powell and S.-W. Du, *Eur. J. Inorg. Chem.*, 2013, 5534.
- 24 Sugiarto, Y. Imai and Y. Hayashi, *Inorg. Chem.*, 2023, **62**, 1845.
- 25 Q. Yin, J. M. Tan, C. Besson, Y. V. Geletii, D. G. Musaev, A. E. Kuznetsov, Z. Luo, K. I. Hardcastle and C. L. Hill, *Science*, 2010, **328**, 342–345.
- 26 H. Lv, J. Song, Y. V. Geletii, J. W. Vicks, J. M. Sumliner, D. G. Musaev, P. Kögerler, P. F. Zhuk, J. Bacsá, G. Zhu and C. L. Hill, *J. Am. Chem. Soc.*, 2014, **136**, 9268.
- 27 Y. Kikukawa, K. Suzuki, K. Yamaguchi and N. Mizuno, *Inorg. Chem.*, 2013, **52**, 8644.
- 28 Y. Kuriyama, Y. Kikukawa, K. Suzuki, K. Yamaguchi and N. Mizuno, *Chem. – Eur. J.*, 2016, **22**, 3962.
- 29 D. Altermatt and I. D. Brown, *Acta Crystallogr.*, 1985, **B41**, 244.
- 30 D. Griller and K. U. Ingold, *Acc. Chem. Res.*, 1980, **13**, 317.
- 31 Y. Kikukawa, Y. Sakamoto, H. Hirasawa, Y. Kurimoto, H. Iwai and Y. Hayashi, *Catal. Sci. Technol.*, 2022, **12**, 2438.
- 32 H. Nakano, T. Ozeki and A. Yagasaki, *Acta Crystallogr.*, 2002, **C58**, m464.
- 33 I. Yoshida, Y. Kikukawa, R. Mitsuhashi and Y. Hayashi, *Nanoscale*, 2024, **16**, 10584.